Nonthermal hot dark matter from inflaton or moduli decay: Momentum distribution and relaxation of the cosmological mass bound

Sukannya Bhattacharya,[1,*] Subinoy Das,[2,†] Koushik Dutta,[3,4,‡] Mayukh Raj Gangopadhyay,[5,§] Ratul Mahanta,[6,‖] and Anshuman Maharana[6,¶]

[1]*Theoretical Physics Division, Physical Research Laboratory, Navrangpura, Ahmedabad—380009, India*
[2]*Indian Institute of Astrophysics, Bengaluru, Karnataka 560034, India*
[3]*Indian Institute of Science Education And Research Kolkata, Mohanpur, WB 741 246, India*
[4]*Theory Division, Saha Institute of Nuclear Physics, HBNI, Kolkata-700064, India*
[5]*Centre for Theoretical Physics, Jamia Millia Islamia, New Delhi 110025, India*
[6]*Harish-Chandra Research Institute, HBNI, Allahabad 211019, India*

(Received 17 October 2020; accepted 12 February 2021; published 4 March 2021)

Decay of the inflaton or moduli which dominated the energy density of the universe at early times leads to a matter to radiation transition epoch. We consider nonthermal sterile dark matter (DM) particles produced as decay product during such transitions. The particles have a characteristic energy distribution—that associated with decays taking place in a matter dominated universe evolving to radiation domination. We primarily focus on the case when the particles are hot dark matter, and study their effects on the cosmic microwave background (CMB) and large scale structure (LSS), explicitly taking into account their nonthermal momentum distribution. Our results for CMB angular power and linear matter power spectra reveal interesting features—such as an order of magnitude higher values of hot dark matter mass in comparison to the thermal case being consistent with the present data. We observe that this is related to the fact that $\Delta N_{\rm eff}$ (the effective number of relativistic degrees of freedom at the time of CMB decoupling) and the hot DM energy density can be independent of each other unlike the case of thermal or nonresonantly produced sterile hot DM. We also find features in the CMB at low ℓ angular power potentially related to supersonic transmission of hot dark matter through the photon-baryon plasma.

DOI: 10.1103/PhysRevD.103.063503

I. INTRODUCTION

Understanding the nature of dark matter is a central question in both particle physics and cosmology. The physics of a constituent species of dark matter not only depends on its mass and interactions but also on its momentum distribution function. For species that thermalize, the momentum distribution is either Fermi-Dirac or Bose-Einstein. On the other hand, for nonthermal constituents the momentum distribution crucially depends on their production mechanism. Thus, as we enter the era of precision cosmology, it is important to isolate natural production mechanisms for dark matter constituents, the associated momentum distributions, and explore their implications [1].

From the point of view of theoretical models, it is natural for the early universe to enter an epoch of matter domination. The inflationary paradigm has emerged as the leading candidate for providing an explanation for the fluctuations in the CMB and the matter power spectrum. In this context, if the inflaton decays perturbatively, then the reheating epoch is matter dominated with cold inflaton particles dominating the energy density of the universe [2]. Furthermore, in string and supergravity models, an epoch of early matter domination arising from vacuum misalignment of moduli fields is a generic feature [3–6] (see, e.g., [7,8] for reviews). An epoch of matter domination ends with the decay of the associated cold particles. This decay process effectively provides a set of initial conditions for the evolution of the universe. For decay products that thermalize, thermalization leads to loss of all information about the kinematics of the decay process. But in a setting with a large number of hidden sectors (which is the generic expectation in string theory [9]) one can expect that some of the species produced during the decay do not thermalize due to very weak interactions. In this case, the energy distribution of the species takes a characteristic (nonthermal) form—that associated with the kinematics of decays taking place in a matter dominated universe evolving into a radiation dominated universe (with the matter to radiation transition taking place as a result of the decay). This energy distribution from decays in such

*sukannya@prl.res.in
†subinoy@iiap.res.in
‡koushik.physics@gmail.com
§mayukh@ctp-jamia.res.in
‖ratulmahanta@hri.res.in
¶anshumanmaharana@hri.res.in

transition epochs has been studied in the context of primordial nucleosynthesis in [10], in the context of moduli decaying to light axions in [11]. We consider the scenario where the decaying particle decays to the Standard Model sector and the sterile particles. But the sterile particle is decoupled from the SM plasma from the very beginning and keeps free-streaming all the way to the present epoch.

As described above, a well-motivated setting for the production of nonthermal constituents is during the matter to radiation transition epoch, with sterile particles being one of the decay products. The goal of this paper is to study the precise implications for the cosmic microwave background (CMB) and large scale structure (LSS) of sterile hot dark matter produced by this mechanism. A key input for this is the momentum distribution today of the sterile particles produced. We obtain this from the energy distribution computed in [10,11]. The momentum distribution depends on the mass of the decaying particle, its half life and the branching ratio for the decay to the sterile particles. In this paper, we treat these quantities and the mass of the sterile particles produced as phenomenological parameters while studying the cosmological implications making use of the publicly available package CLASS [12–14].

We will focus on the case in which the sterile particles produced from the decay of inflaton/moduli act as hot dark matter that constitutes a small fraction of the total dark matter density today. Recall that though a sterile particle/neutrino with higher mass $m \gtrsim 5$ keV is a viable warm dark matter candidate [15–24], a lighter fermion (hot dark matter) with $m \sim$ eV usually falls into the dark-matter misfortune as eV mass particle free-streams until relatively late times in cosmic evolution and erases structure on small scales. Only a small fraction of the dark matter abundance can be in the form of neutrinos or other light species with $m \sim$ eV and this puts a stringent upper bound on neutrino mass [25].[1] On the other hand, recent data from MiniBooNE experiment might indicate the existence of light sterile neutrino states of $\sim$(1–10) eV [28]. Within the "3 + 1" neutrino oscillation framework, these results are, however, very difficult to reconcile with the absence of anomalies in the $\nu_\mu \to \nu_\mu$ disappearance as probed by recent atmospheric [29] and short baseline [30] experiments. If these results are confirmed by future analyses, it is likely that new physics beyond the (sterile + active) oscillation models would be necessary to resolve the tension between neutrino appearance and disappearance data.

Cosmology provides a complementary means to probe eV scale neutrino/hot DM particles. Cosmological observables such as the CMB and large-scale structure (LSS) are also sensitive to the presence of new interactions [31,32] in the neutrino sector that would modify their standard free-streaming behavior during the radiation-dominated epoch. As shown in [31], this would change the hot DM mass bound as well put constraints on effective radiation degree of freedom $\Delta N_{\rm eff}$. Another important factor is whether the light sterile neutrinos are fully thermalized or not. Not only that a nonthermal distribution function would have implications for short baseline anomaly [33] but also hot DM mass bound and its effective contribution to the radiation energy density would change considerably [34–37]. The subject of hot dark matter in cosmology has a vast body of literature, the reader might find the papers [34,37–82] and the references therein interesting in the context of the present work. More specifically, the paper [38] initiated the study of hot/warm dark matter from decays. For general overviews, see, e.g., [76,83–87].

For our analysis, we consider what seems to us as a simple and well-motivated setting. The decaying particle (φ) is the inflaton with mass $m_\varphi \sim 10^{-6} M_{\rm pl}$. We take its lifetime to be of the order of $10^8/m_\varphi$ to $10^9/m_\varphi$. This can arise if the decay takes place via a nonrenormalizable interaction at approximately the GUT scale. Interestingly, we find that in this regime of parameter space the mass of this candidate hot dark matter particles can be significantly higher than the standard thermal hot dark matter case and still be consistent with data (we discuss the regime of parameter space where there can be significant observable effects in Sec. III). Another interesting aspect is the ℓ dependence of the effects on the CMB. For large ℓ, the main effect is from $\Delta N_{\rm eff}$ as it changes the Hubble expansion rate prior to photon decoupling which changes the silk damping scale [88]. As our hot DM particle increases $\Delta N_{\rm eff}$, we also see the expected suppression in power on large ℓCMB angular power spectra. It is instructive to note that we fix our decay parameters to the range of values which obey Planck bound of $\Delta N_{\rm eff}$. For lower values of ℓ, the effects due to supersonic transmission of hot dark matter through the photon-baryon plasma can be important [31]. Future MCMC analysis (work in progress) will make these effects more clear and would shed light whether one can detect these subtle effects of nonthermal hot DM produced from early decay through future CMB experiments.

This paper is structured as follows. In Sec. II, we obtain the momentum distribution function of sterile particles produced from decay during a matter to radiation transition epoch. In Sec. III, we begin by briefly reviewing the effects that hot dark matter can have on the CMB and LSS. We then go on to input the momentum distribution function to CLASS and obtain our results. Finally in Sec. IV, we discuss future directions and conclude.

II. STERILE DECAY PRODUCTS AND THE ASSOCIATED MOMENTUM DISTRIBUTION FUNCTION

In our scenario, the sterile particles are produced from the decay of a heavy massive scalar (φ) We consider $1 \to 2$

[1] But as the neutrino has all the relevant properties of DM, except free-streaming, there have been efforts to revive the neutrino or lighter sterile neutrino as viable dark matter candidate with nontrivial cosmological histories or exotic interactions [26,27].

decays, with identical decay products. The production takes place in the early universe, when φ is decaying and the universe is in a matter to radiation transition epoch. The species φ decays to the sterile particle with branching ratio $B_{\rm sp}$, these particles do not thermalize. The remaining decay products thermalize (as this sector contains the Standard Model, we will refer to this as the Standard Model sector).

The momentum distribution of the sterile particles is central to obtain their effect on the CMB and LSS. To compute this momentum distribution, one needs to know the scale factor of the universe during the epoch that φ decays. Thus, we start by discussing the evolution of the scale factor during this epoch [2,11].

A. The scale factor

The evolution of the universe during the epoch that φ decays is governed by the equations:

$$\dot{\rho}_{\rm mat} + 3H\rho_{\rm mat} = -\frac{\rho_{\rm mat}}{\tau}, \tag{1}$$

$$\dot{\rho}_{\rm rad} + 4H\rho_{\rm rad} = +\frac{\rho_{\rm mat}}{\tau}, \tag{2}$$

and

$$H = \left(\frac{\dot{a}}{a}\right) = \sqrt{\frac{\rho_{\rm mat} + \rho_{\rm rad}}{3M_{\rm pl}^2}}. \tag{3}$$

In the above, $\rho_{\rm mat}$ denotes the energy density in matter and $\rho_{\rm rad}$ is the energy density in radiation. Here, τ represents the lifetime of the φ particles. The energy density in radiation is the sum of the energy densities in the Standard Model sector and sterile particles (since the sterile particles are highly relativistic at the time of production, thus they contribute to the energy density as radiation during the epoch that φ decays). It is useful to introduce the dimensionless variables

$$\theta = \frac{t}{\tau}, \qquad \hat{s}(\theta) = a(\tau\theta), \quad \text{and}$$
$$e_{\rm mat}(\theta) = \frac{\tau^2\rho_{\rm mat}(\tau\theta)}{M_{\rm pl}^2}, \qquad e_{\rm rad}(\theta) = \frac{\tau^2\rho_{\rm rad}(\tau\theta)}{M_{\rm pl}^2}. \tag{4}$$

Now, let us come to the initial conditions. We will take the starting point of our numerical evolutions to be $t = 0$, and work with conventions in which the scale factor is equal to unity at this point. At this stage, the universe is completely matter dominated, thus we will take

$$\rho_{\rm mat}(0) = \frac{4\alpha}{3}\frac{M_{\rm pl}^2}{\tau^2} \quad \text{i.e} \quad e_{\rm mat}(0) = \frac{4}{3}\alpha, \tag{5}$$

with $\alpha \gg 1$ (the factor of $4/3$ has been chosen so as to get some numerical simplifications) and the energy density in radiation to be zero. We note that the solution will be universal[2] in the sense that we will get the same late time universe as long as $\alpha \gg 1$. In our numerics, we will take $\alpha = 10^4$. We exhibit the results of numerical integration of the evolution equations in the form of plots. Figure 1, shows the evolution of the scale factor while Fig. 2 exhibits the energy density in radiation as a function of the dimensionless time θ.

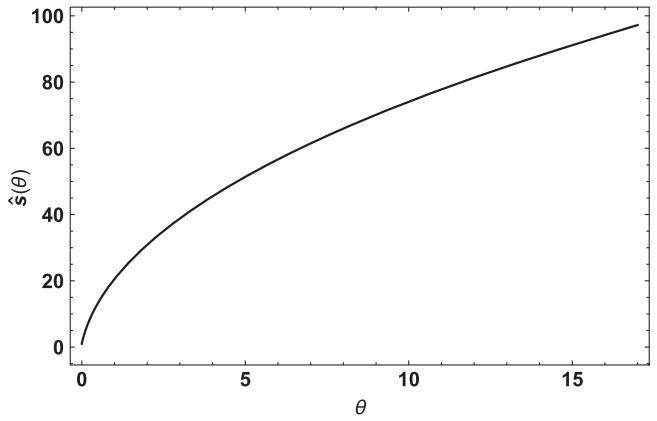

FIG. 1. The scale factor as a function of the dimensionless time.

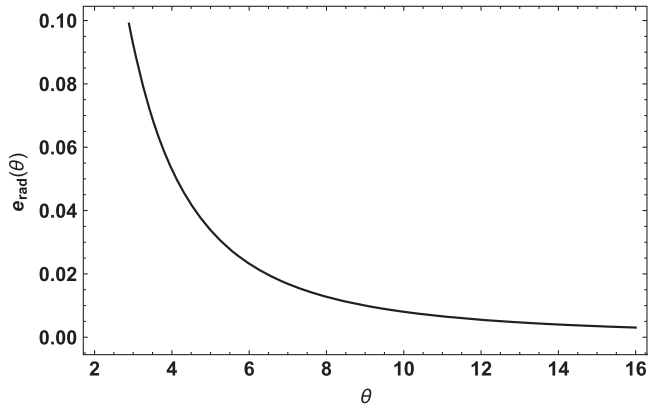

FIG. 2. The energy density in radiation as a function of the dimensionless time.

B. The energy distribution at early times

The timescale for the decay of the φ particles is τ, at these early times the sterile particles produced are highly relativistic. Let us begin by discussing their energy distribution at these early times as obtained in [10,11]. The treatment in [10] is rather brief (the final result of the computation is presented as a plot), we will primarily follow [11]. The comoving modulus number density as function of time is given by

[2]This is a consequence of the fact that for energy densities much greater than $\frac{M_{\rm pl}^2}{\tau^2}$, the Hubble time is much smaller than τ.

$$N = N(0)e^{-t/\tau}, \tag{6}$$

where $N(0)$ is the number density at $t = 0$. Note that $N(0)$ can be computed from (5).

$$N(0) = \frac{\rho_{\rm mat}(0)}{m_\varphi} = \frac{4\alpha M_{\rm pl}^2}{3\tau^2 m_\varphi}. \tag{7}$$

If a sterile particle is produced from decay of a modulus at time $t = t_d$, then at that point of time it has energy $\hat{E} = m_\varphi/2$. At a later time t, its energy is given by[3]

$$E = \hat{E}\left(\frac{a(t_d)}{a(t)}\right).$$

Thus at time t, sterile particles produced between t_d and $t_d + dt_d$ have energies in the range

$$dE = EH(t_d)dt_d. \tag{8}$$

The number density of sterile particles produced between t_d and $t_d + dt_d$ can be computed from (6):

$$dN = \frac{2B_{\rm sp}}{\tau} N(0)e^{-t_d/\tau}dt_d. \tag{9}$$

Equations (8) and (9) can be combined to compute the comoving number density spectrum (as a function of the energy) at time t [11]:

$$dN_t^c = \frac{2B_{\rm sp}}{\tau} N(0)e^{-t_d/\tau}\frac{1}{EH(t_d)}dE. \tag{10}$$

where t_d is to be expressed in terms of t and E, by making use of the relation $E = \hat{E}\frac{a(t_d)}{a(t)}$. The physical number density is obtained by dividing this by $a^3(t)$. Doing this, and converting to our dimensionless variables introduced in (4) one obtains the spectrum at time t to be

$$dN_t = \frac{1}{\hat{s}^3(\theta)} 2N(0)B_{\rm sp}\frac{e^{-\hat{s}^{-1}(y)}}{\hat{H}(\hat{s}^{-1}(y))E}dE \equiv \tilde{n}_t(E)dE. \tag{11}$$

where we have introduced the variable y:

$$y \equiv \frac{E\hat{s}(\theta)}{\hat{E}}, \tag{12}$$

with $\theta = t/\tau$. $\hat{H}$ is the dimensionless Hubble parameter $\hat{H} \equiv \hat{s}'(\theta)/\hat{s}(\theta)$. Finally, $\hat{s}^{-1}$ is the inverse of the scale factor function introduced in (4). We note that the spectrum in (11) is nonvanishing for E in the range $\frac{\hat{E}}{\hat{s}(\theta)} < E < \hat{E}$. The lower limit corresponds to decays at the initial time and upper limit corresponds to decays that at occur at θ. This implies that y varies between 1 and $\hat{s}(\theta)$.

[3]In this subsection we will assume that t is small enough so that the sterile particles continue to be highly relativistic at t.

C. The momentum distribution function today

The discussion in the previous subsection can be used to compute the momentum distribution of the sterile particles today. At early times, the sterile particles are highly relativistic. The momentum distribution can be computed from the energy distribution in (11) using isotropy.

$$dN_t = \frac{\tilde{n}_t(|\vec{p}|)}{4\pi|\vec{p}|^2}d^3p \equiv n_t(\vec{p})d^3p. \tag{13}$$

The momentum distribution today can be obtained by making use of the fact that after production the sterile particles free stream. Thus if t^* is an early time such that almost all the φ particles have decayed by t^*, then the momentum distribution of the sterile particles today is given by

$$n_{t_0}(\vec{p}) = n_{t^*}\left(\frac{a(t_0)}{a(t^*)}\vec{p}\right). \tag{14}$$

Note that given our earlier discussion regarding the values of the argument of $\tilde{n}_t$ for which it is nonvanishing, $n_{t_0}(\vec{p})$ is nonvanishing if

$$\frac{\hat{E}}{a(t_0)} < |\vec{p}| < \frac{\hat{E}a(t^*)}{a(t_0)}. \tag{15}$$

For our numerics, we shall use $t^* = 15\tau$ (i.e $\theta^* = 15$).

The CLASS routine requires that the momentum distribution is expressed in units of $T_{\rm ncdm,0}$, the typical momentum of the dark radiation particles today. Equation (15) gives the range of the momentum for the sterile particles. The range of momentum in (15) corresponds to decays taking between $t = 0$ and $t = 15\tau$, we expect most of the decays to take place in the early part of this range in time. This motivates us to take

$$T_{\rm ncdm,0} = \frac{\hat{E}}{4}\frac{a(t^*)}{a(t_0)} = \frac{1}{8}m_\varphi\left(\frac{g(t_0)}{g(t^*)}\right)^{\frac{1}{3}}\left(\frac{T(t_0)}{T(t^*)}\right). \tag{16}$$

$T(t^*)$, the temperature of the Standard Model sector at t^* can be computed from numerical analysis of the evolution of the energy density in radiation carried out in Sec, II A. The energy density in the Standard Model sector at t^* is

$$\rho_{\rm sm}(t^*) = \frac{M_{\rm pl}^2}{\tau^2}(1 - B_{\rm sp})e_{\rm rad}(\theta^*), \tag{17}$$

Thus the temperature of the plasma at $t = t^*$ is

$$T(t^*) = \left(\frac{3}{4}e_{\rm rad}(\theta^*)\right)^{1/4}\left(\frac{40(1-B_{\rm sp})}{\pi^2 g_*(T(t^*))}\right)^{1/4}\left(\frac{M_{\rm pl}}{\tau}\right)^{1/2}. \tag{18}$$

Our numerics in Sec. II A give $(\frac{3}{4})^{1/4}(e_{\rm rad}(15))^{1/4} = 0.2262$. Now, taking $g(t_0) = 3.91$ and $g(t^*) \sim 100$ in (18), we obtain

$$T_{\rm ncdm,0} = 0.418\left(\frac{m_\varphi^2\tau}{M_{\rm pl}}\right)^{1/2}\frac{T_{\rm cmb}}{(1-B_{\rm sp})^{1/4}} \equiv \zeta T_{\rm cmb}, \quad (19)$$

where we have defined $\zeta = \frac{0.418}{(1-B_{\rm sp})^{1/4}}(\frac{m_\varphi^2\tau}{M_{\rm pl}})^{1/2}$. Finally, we express the momentum distribution function in terms of the momentum is units of $T_{\rm ncdm,0}$,

$$q \equiv \frac{|\vec{p}|}{T_{\rm ncdm,0}}. \quad (20)$$

Making this variable change, (13) gives the momentum distribution in units of $(T_{\rm ncdm,0})^3$ to be

$$f(q) = \frac{32}{\pi\hat{E}^3}\left(\frac{N(0)B_{\rm sp}}{\hat{s}^3(\theta^*)}\right)\frac{e^{-\hat{s}^{-1}(y)}}{q^3\hat{H}(\hat{s}^{-1}(y))}, \quad (21)$$

where

$$y = \frac{q}{4}\hat{s}(\theta^*), \quad (22)$$

and the range of q is given by

$$\frac{4}{\hat{s}(\theta^*)} < q < 4. \quad (23)$$

III. EFFECTS ON COSMOLOGICAL OBSERVABLES

In this section, we carry out our analysis on the cosmological observables making use of the above discussed nonthermal momentum distribution function. Let us begin by briefly reviewing the key effects that such particles can have on cosmology. For a more detailed discussion see e.g [83].

A. Review of effects of hot DM on cosmology

Hot DM neutrinolike particles have significant effect on the expansion rate during the cosmological era when the Universe is radiation dominated. Their contribution to the total radiation content can be parametrized in terms of $N_{\rm eff}$. Other than changing the expansion rate of the Universe, another important effect is free-streaming of hot DM until they turn nonrelativistic. The physical effect of free-streaming is to damp small-scale density fluctuations: hot DM cannot be confined into regions smaller than their free-streaming length, because their velocity is greater than the escape velocity from gravitational potential wells on those scales. On the other hand, on scales much larger than the free-streaming scale, their velocity can be effectively considered as vanishing, and after the nonrelativistic transition the hot DM perturbations behave like CDM perturbations.

1. Effect of hot eV mass dark matter on matter power spectrum

On large scales (i.e on wave-numbers smaller than k_{nr}), the matter power spectrum $P(k,z)$ can be shown to depend only on the matter density fraction Ω_m today (including neutrinos which was hot earlier but now behaves like CDM). Here, k_{nr} represents the scale associated with the time at which the DM becomes non relativistic. If the hot DM mass is varied with Ω_m fixed, the large scale power spectrum remains invariant but on small scales $k > k_{nr}$, the matter power spectrum is affected by hot DM masses for essentially three reasons:

(1) Massive hot DM does not cluster on those scales. The matter power spectrum can be written as,

$$P(k,z) = \left\langle\left|\frac{\delta\rho_{\rm cdm}+\delta\rho_{\rm b}+\delta\rho_{sp}}{\rho_{\rm cdm}+\rho_{\rm b}+\rho_{sp}}\right|^2\right\rangle = \Omega_{\rm m}^{-2}\langle|\Omega_{\rm cdm}\delta_{\rm cdm}+\Omega_{\rm b}\delta_{\rm b}+\Omega_{sp}\delta_{sp}|^2\rangle. \quad (24)$$

where $\delta\rho_{sp}$ and Ω_{sp} represents density fluctuation and fractional energy density of our sterile particle (hot DM). On scales of interest and in the recent universe, baryon and CDM fluctuations are almost equal to each other, while $\delta_{sp} \ll \delta_{\rm cdm}$. The power spectrum would be reduced by a factor $(1-f_{sp})^2$ with

$$f_{sp} \equiv \frac{\Omega_{sp}}{\Omega_{\rm m}}. \quad (25)$$

(2) The redshift of radiation-to-matter equality $z_{\rm eq}$ or the baryon-to-CDM ratio $\omega_{\rm b}/\omega_{\rm cdm}$ can be slightly affected by sterile particle masses, with a potential impact on the small-scale matter power spectrum. This depends on which other parameters are kept fixed when the sterile particle hotDM mass is varied. But matter power spectra also can be affected by perturbative cosmology in presence of hot Dark matter.

(3) The growth rate of cold dark matter perturbations is reduced through an absence of gravitational back-reaction effects from free-streaming hot DM. This growth rate is set by an equation of the form

$$\delta''_{\rm cdm} + \frac{a'}{a}\delta_{\rm cdm} = -k^2\psi, \quad (26)$$

where $\delta_{\rm cdm}$ stands for the CDM relative density perturbation in Fourier space, and ψ for the metric perturbation playing the role of the Newtonian

potential inside the Hubble radius. The right-hand side represents gravitational clustering. The second term on the left-hand side represents Hubble friction, i.e., the fact that the cosmological expansion slows down clustering. The coefficient a'/a is given by the first Friedmann equation as a function of the total background energy density. In a universe such that all species present in the Friedmann equation do cluster, as it is the case in a matter-dominated universe with $\delta\rho_{\rm total} \simeq \delta\rho_{\rm cdm} + \delta\rho_b$ and $\bar{\rho}_{\rm total} = \bar{\rho}_{\rm cdm} + \bar{\rho}_{\rm b}$, the solution is simply given by $\delta_{\rm cdm} \propto a$: the so-called linear growth factor is proportional to the scale factor. But whenever one of the species contributing to the background expansion (like our sterile particle) does not cluster efficiently, the CDM (as well as baryons) clusters at a slower rate. This is why measuring linear matter power spectra put strong bounds on hot dark matter mass.

2. Effect of hot dark matter on CMB

The implications for the CMB can summarized by the following three effects:

(1) Hot dark matter can affect the redshift of matter/radiation equality $z_{\rm eq}$ via its contribution to $\rho_{\rm m}$ and ρ_r which depend on its mass. If they are relativistic at $z_{\rm rec}$ then it is reasonable to assume that they contribute only to $\rho_{\rm rad}$, though they could be mildly relativistic near $z_{\rm eq}$. This can modify the contribution from the early ISW effect and have an effect on the CMB.

(2) Hot dark matter changes the expansion rate by changing the energy density, this in turn changes the size of the sound horizon at recombination and/or the distance to last scattering. Changes in the expansion rate can also affect the damping scale and this is one of the main effects how an excess radiation affects CMB [88].

(iii) Free-streaming sterile particle (or hot dark matter) can travel supersonically through the photon-baryon plasma at early times, hence gravitationally pulling photon-baryon wavefronts slightly ahead of where they would be in the absence of hot DM. As a result, free-streaming hot DM imprints a net phase shift in the CMB power spectra at larger scales (smaller ℓ), as well as a slight suppression of the amplitude. This phase shift is considered to be a robust signature of the presence of free-streaming radiation in the early Universe.

The total relativistic energy density of the Universe at late time is parametrized by $N_{\rm eff}$, where $\Delta N_{\rm eff} = N_{\rm eff} - 3.046$ corresponds to additional dark relativistic degrees of freedom other than the three neutrino flavours of the SM. In our case, the massive sterile particle with its characteristic nonthermal distribution contributes to dark radiation. In this case, the bound is conventionally characterized by $m^{\rm eff}_{X,\rm sterile} \equiv \Omega_{X,\rm sterile} h^2 (94.1\ {\rm eV})$ and $N_{\rm eff}$, where $m^{\rm eff}_{X,\rm sterile}$ is related to the physical mass of the sterile particle and the relation differs for different models. The latest PLANCK + BAO bounds on these parameters are as follows: $N_{\rm eff} < 3.29$, $m^{\rm eff}_{X,\rm sterile} < 0.65$ eV [25]. From this bound, it is clear that hot dark matter can only constitute a very small fraction of the total dark matter energy density.

B. Finding CMB and LSS observables for our nonthermal hot dark matter

Keeping the above effects in mind and having obtained the momentum distribution of the sterile particles, in this section we will compute their effect on LSS and the CMB. The full computation for this will be done numerically by modifying the publicly available CLASS code [12,13] to incorporate the new distribution function. It is important to keep in mind that while the full computation takes the momentum distribution as input and has to be done numerically, the effect on the CMB and LSS are primarily set by three parameters which can be easily calculated once the momentum distribution is known [35]. These are

(1) $\Delta N_{\rm eff}$: The number of additional relativistic species at the time of neutrino decoupling (the sterile particles are relativistic at this point). Current bounds require $\Delta N_{\rm eff} \lesssim 0.3$, [25]. In our case, the sterile particles and the Standard Model sector are both entirely produced from the decay of φ particles. Thus, the relative energy densities of the two sectors at early times is $B_{\rm sp}/(1 - B_{\rm sp})$. Given this, $\Delta N_{\rm eff}$ is easily computed by standard methods, see e.g [11,89–91]. One finds[4]

$$\Delta N_{\rm eff} = \frac{43}{7} \frac{B_{\rm sp}}{1 - B_{\rm sp}} \frac{(g_*(T(t_\nu))^{1/3}}{g_*(T(t^*)))}, \qquad (27)$$

where t_ν is the time at which neutrinos decouple.

(2) $\lambda_{\rm FS}$: Till the epoch when hot dark matter particles turn nonrelativistic, they cannot be bound in gravitational potential wells of cold dark matter. The comoving distance traveled by hot DM particles till the temperature of the universe drops below their mass is known as the free streaming length. As hot DM (which is cold at the present epoch) contributes to a fraction of entire dark matter budget today, due to this early free streaming behavior, the linear matter power spectra generally gets suppressed at length scales smaller than $\lambda_{\rm FS}$. Hot dark matter turns nonrelativistic deep in the matter dominated era. A quick estimate[5] of the minimum free streaming wave

[4]This assumes instantaneous thermalization of the Standard Model sector [11].

[5]CLASS computes the exact free streaming wavelength directly from the momentum distribution, the estimate we give is only for the purposes of the present discussion.

number in our case can be obtained following [83]. We find

$$k_{\rm fs} \approx 0.018 \left(\frac{m_{\rm sp} T_\nu}{\zeta T_{\rm cmb} 1\,{\rm eV}}\right)^{1/2} (\Omega_m h)^{1/2}\,{\rm Mpc}^{-1}, \quad (28)$$

with ζ as defined in (19).

(3) $w_{\rm sp}$: which is related to the current energy density of the sterile particle (the product of its current number density and its mass). Following the conventions of [35], we will take

$$w_{\rm sp} = m_{\rm sp} n_{\rm sp} \left[\frac{h^2}{\rho_c^0}\right], \quad (29)$$

where $m_{\rm sp}$ and $n_{\rm sp}$ are the mass and number density of the sterile particle. ρ_c^0 is the critical density today and h is the reduced Hubble parameter. To compute $w_{\rm sp}$, we need to compute $n_{\rm sp}$, the number density of the sterile particles today. To do this, we begin by computing the abundance (Y) of the particles. The energy density of the standard model sector at t^* is

$$\begin{aligned}\rho_{\rm sm}(t^*) &= (1 - B_{\rm sp})\rho_{\rm rad}(15\tau) \\ &= (1 - B_{\rm sp})\frac{M_{\rm pl}^2}{\tau^2} e_{\rm rad}(15) \end{aligned} \quad (30)$$

Thus the entropy density at this point is

$$\begin{aligned} s(15\tau) = &\left(\frac{3}{4} e_{\rm rad}(15)\right)^{3/4} \left(\frac{4}{3}\right) \left(\frac{\pi^2}{30}\right)^{1/4} \\ &\times g_*^{1/4}(T(t^*)) \left(\frac{M_{\rm pl}}{\tau}\right)^{3/2}. \end{aligned} \quad (31)$$

The number density at t^* can be computed similarly. The number density at the initial time is given in (7) By $t = t^*$, almost all the φ particles decay; their branching fraction to the sterile particles is $B_{\rm sp}$. Thus, to a very good approximation the number density of the sterile particles at $t = t^*$ is

$$n(15\tau) = \frac{2 B_{\rm sp} N(0)}{a^3(15\tau)}. \quad (32)$$

Now computing the abundance by taking the ratio of (31) and (32), and using this to compute the number density of the sterile particles in terms of number density of neutrinos today (n_ν) today we find

$$\begin{aligned} n_{\rm sp} = 1.13 &\left[\frac{43\pi^4}{45.3.\zeta(3)}\right] \frac{3}{\pi^{1/2} g_*^{1/4}(T(t^*))} \left(\frac{5}{2}\right)^{1/4} \\ &\times \frac{B_{\rm sp}}{(1 - B_{\rm sp})^{3/4}} \left(\frac{M_{\rm pl}}{\tau m_\varphi^2}\right)^{1/2} n_\nu. \end{aligned} \quad (33)$$

From this, the parameter $w_{\rm sp}$ [as defined (29)] is found to be

$$w_{\rm sp} = \frac{m_{\rm sp}}{94.05\ {\rm eV}} \frac{62.1}{g_*^{1/4}(T(t^*))} \frac{B_{\rm sp}}{(1 - B_{\rm sp})^{3/4}} \left(\frac{M_{\rm pl}}{\tau m_\varphi^2}\right)^{1/2}. \quad (34)$$

A few comments are in order:

(i) In the computation of $w_{\rm sp}$, various intermediate expressions depend on α (the dimensionless energy density at the initial time). We have checked $w_{\rm sp}$ is independent of this choice for the initial energy density, as long as $\alpha \gg 1$. This is in keeping with the expectation that for $\alpha \gg 1$, the late time solution is universal.

(ii) It is interesting to compare the expression (34) for $w_{\rm sp}$ with that for the same in the instantaneous decay approximation, the primary focus of [38,39]. While the functional dependence on the various parameters is the same, the overall coefficient is greater by a factor of approximately fifteen percent. This exhibits the importance of incorporating the exact background and the associated distribution function.

1. Results of numerics

CLASS (cosmic linear anisotropy solving system) [12] is a numerical code which simulates the evolution of the background and perturbations of the universe working to the linear order. The inputs for the default code are the present day values of different cosmological parameters ($\Omega_b^{(0)} h^2$, $\Omega_c^{(0)} h^2$, H_0, primordial parameters from inflation etc.) for the 6-parameter ΛCDM model and its extensions. The outputs are typically the observables for CMB and LSS experiments, i.e., the temperature power spectrum of the CMB (C_ℓ^{TT}), temperature-polarization power spectra (C_ℓ^{TE}) and the matter power spectrum ($P(k)$) etc.

Working with an extension of the 6-parameter ΛCDM model, here we include the mass ($m_{\rm SP}$) and momentum distribution $f(q)$ of an additional component of hot dark matter as inputs [13]. We emphasize that in our implementation we explicitly use the nonthermal distribution function in (21), this is done using the routine described in [14]. The nonthermal momentum distribution $f(q)$ in our case depends on the mass m_φ and lifetime τ of the decaying particle and therefore, we consider few benchmark points to arrive at $f(q)$. Here we note that Ref. [39] suggested that for implementation in CLASS thermal distributions should be used,[6] we disagree as the precise from of the distribution function is absolutely necessary for extracting the predictions from CLASS.

[6]Although [39] did not extract the predictions for the CMB and LSS using CLASS, it outlined a strategy for doing so.

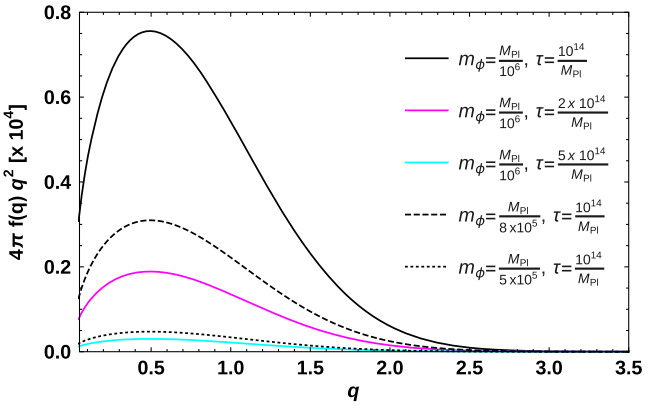

FIG. 3. This figure shows the dependence of the nonthermal momentum distribution on m_φ and τ. In all cases, q and $f(q)$ are in units of the appropriate powers of the associated $T_{\mathrm{ncdm},0}$.

We can use the analytic expression obtained for ΔN_{eff} and w_{sp} to obtain benchmark points for our inputs to CLASS. Note that (27) implies that ΔN_{eff} is essentially determined by the branching ratio B_{sp}. Given the bound $\Delta N_{\mathrm{eff}} \lesssim 0.3$, we take $B_{\mathrm{sp}} = 0.05$. This corresponds to $\Delta N_{\mathrm{eff}} = 0.15$. Now, as described in the introduction, in our scenario it is natural to think of φ as the inflaton. Motivated by this we take $m_\varphi = 10^{-6} M_{\mathrm{pl}}$. We will take the lifetime of the φ as a phenomenological parameter, and consider the points $\tau = 10^8/m_\varphi$ and $\tau = 10^9/m_\varphi$. If the inflaton decays by a nonrenormalizable interaction, then our choice for the lifetime corresponds decay via an interaction suppressed by approximately the GUT scale. In Fig. 3, we plot our distribution function for various values of m_φ and τ. We would also like to comment on the case that φ is a modulus which decays by Planck suppressed interactions. For moduli masses in the range 10^6–10^7 GeV (as considered in [11]), $(\frac{M_{\mathrm{pl}}}{m_\varphi^2 \tau})^{1/2} \sim 10^{-6}$. This makes the effective mass very small (which can be computed using (34) and footnote 7). The effect of the species is then same as that of massless dark radiation which is well understood. For interesting effects the modulus mass has to be high and the phenomenology is similar to that of the above described inflaton case.

It is interesting to compare our nonthermal distribution function with a thermal distribution function for sterile neutrinos with the same value of ΔN_{eff}. We do this in figure 4. Note that our distribution function has a much

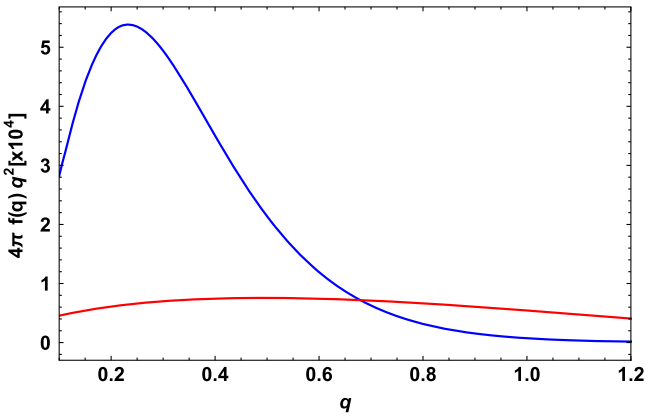

FIG. 4. Comparison with a thermal distribution with the same value of $\Delta N_{\mathrm{eff}} (= 0.15)$. The nonthermal distribution here is for $m_\varphi = 10^{-6} M_{\mathrm{pl}}$, $\tau = 10^8/m_\varphi$ and is plotted in orange. The thermal distribution is in blue. The momenta and the distribution functions for both plots are in units of $T_{\mathrm{ncdm},0}$ for the above value of m_φ and τ.

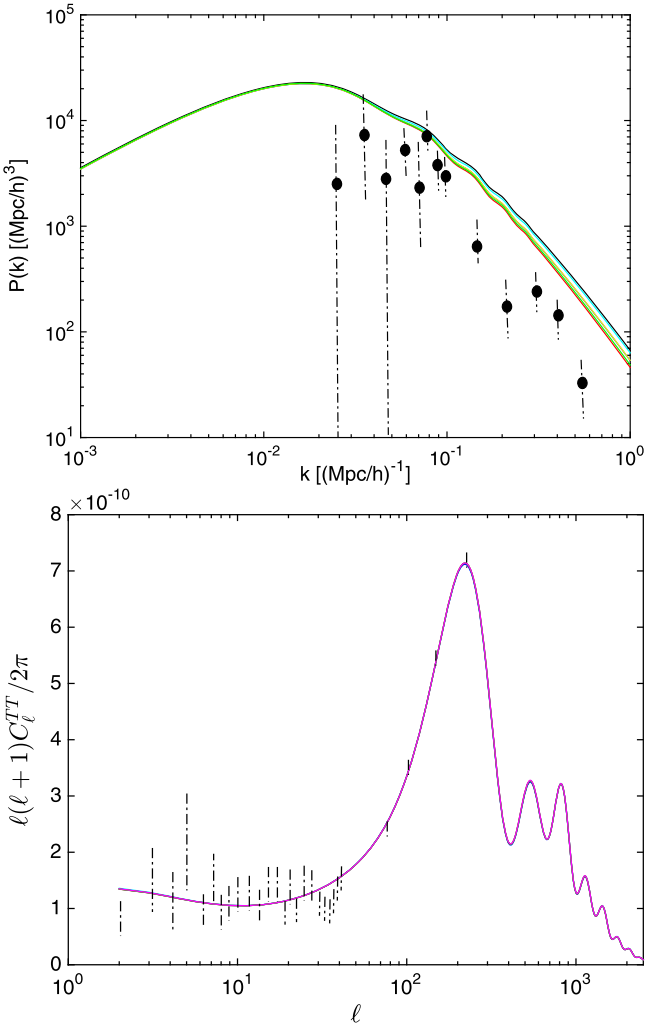

FIG. 5. Upper panel shows full matter power spectra $P(k)$ for $\tau = 10^8/m_\varphi$ with inclusion of SN and SP of different masses. Colour schemes for different scenarios are the same as Fig. 6. Central values and error bars for the WiggleZ experiment are also given in black bold point and dot-dashed lines respectively on top of theoretical plots. The lower panel shows temperature power spectra C_ℓ^{TT} for the same benchmark point with error bars from Planck 2018. θ_* is kept fixed in all the CLASS runs at the Planck 2018 TT + lowP value.

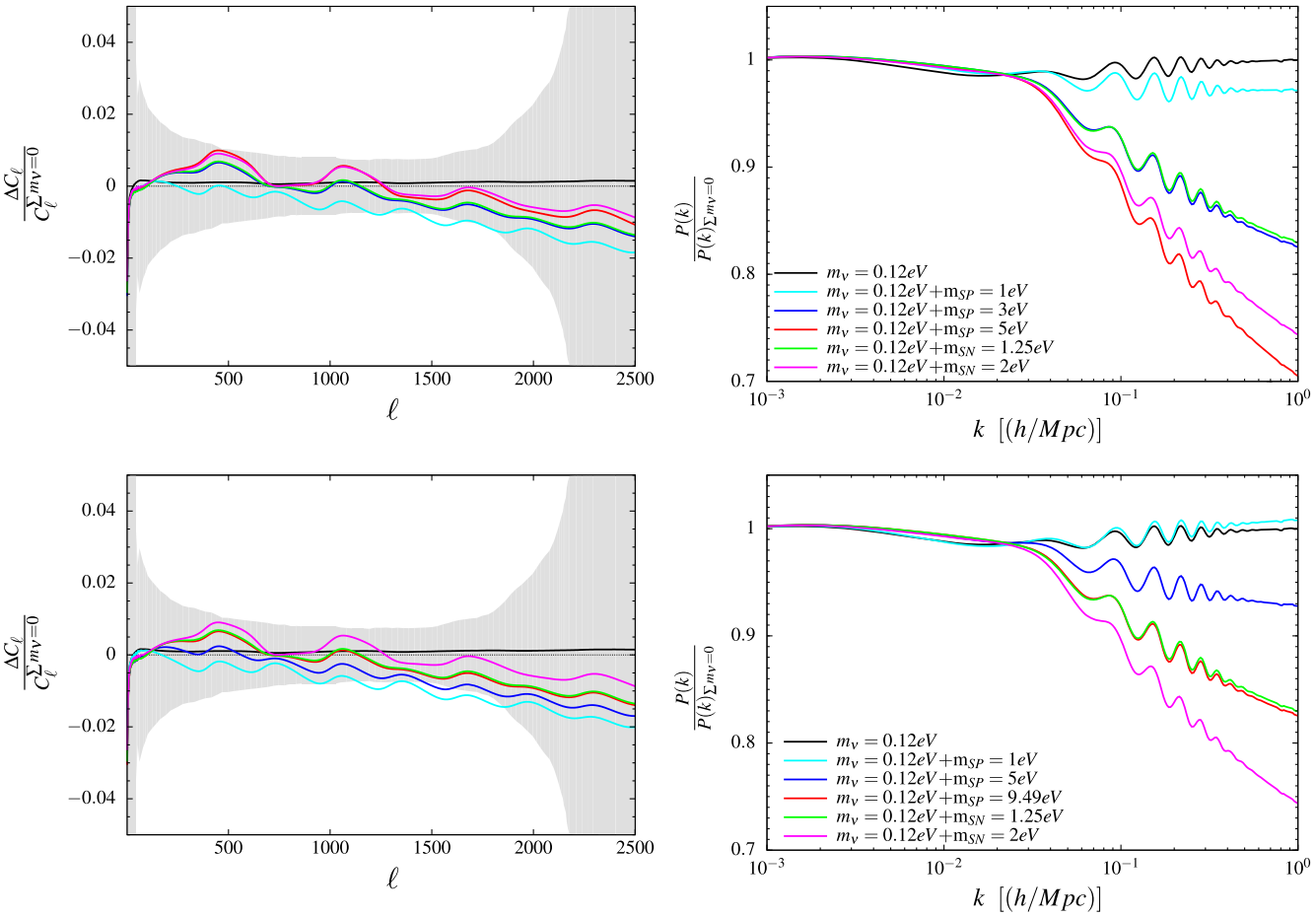

FIG. 6. Fractional deviation of the CMB temperature power spectra C_ℓ^{TT} (left panel) and fractional matter power spectra $P(k)$ (right panel) for different cases including sterile particles (SP) and sterile neutrino (SN) as shown in plot legends. For each case, C_ℓ^{TT} and $P(k)$ are evaluated for $\sum m_\nu = 0.12$ eV + SP/SN and compared to the case where $\sum m_\nu = 0$ with no extra SP or SN species. The upper panels correspond to $\tau = 10^8/m_\varphi$ and the lower panels are for $\tau = 10^9/m_\varphi$. Note that for $\tau = 10^9/m_\varphi$, our hot dark matter at 9.49 eV is equivalent to a 1.25 eV thermalized neutrino (its temperature has been chosen such that both of them have the same $\Delta N_{\rm eff}$). The gray shaded region in the left panel corresponds to observed errors in C_ℓ^{TT} (Planck 2018).

lower maximum value but is much broader than the thermal one.

Taking these as inputs for CLASS we have computed the matter power spectra $P(k)$ and temperature power spectra C_ℓ for the above discussed benchmark points for various values of $m_{\rm sp}$. In addition, for comparison we have plotted the effects of giving the standard model neutrinos a mass or sterile neutrinos (SN) at various masses. The distribution for standard model neutrinos is taken to be thermal in the instantaneous decoupling approximation $T_\nu = (4/13)^{1/3} T_{\rm cmb,0} \simeq 0.17$ meV. The SN are taken to be thermal with a temperature such that their contribution to $\Delta N_{\rm eff}$ is same as that for our benchmark points (i.e $\Delta N_{\rm eff} = 0.15$). For each of the benchmark points, the $T_{\rm ncdm,0}$ is calculated from (19); i.e $T_{\rm ncdm,0} = 4.23 T_{\rm cmb,0} \simeq 1$ meV for $\tau = 10^8/m_\varphi$ and $T_{\rm ncdm,0} = 13.39 T_{\rm cmb,0} \simeq 3.14$ meV for $\tau = 10^9/m_\varphi$ which are then fed in the CLASS code. To keep the redshift $z_{\rm eq}$ of matter-radiation equality consistent at $z_{\rm eq} \simeq 3410$ for all these cases, the value of $\Omega_{\rm c}^{(0)}$ was modified slightly for each case. The outcomes for $P(k)$ from CLASS are plotted in Figure 5. The fractional changes in $P(k)$ and C_ℓ for such cases with respect to the case with no sterile particle with $\sum m_\nu = 0$ are shown in Fig. 6. Now, we discuss two interesting aspects of our results.

(i) As we can see from Fig. 6, the linear matter power spectra gets much less suppression for our hot dark matter when compared to a standard thermalized neutrino of the same mass. The same is true for the effects in the CMB. For example, for $\tau = 10^9/m_\varphi$, we see that our hot dark matter at 9.49 eV is equivalent to a 1.25 eV thermalized neutrino (as discussed earlier, the temperature has been so chosen such that both of them have the same value of $\Delta N_{\rm eff}$). This matching can be seen for our expression of $w_{\rm sp}$ in (34). For the values corresponding to our benchmark point the effective

mass is seen to be reduced by one order of magnitude.[7] This brings to us an important point. For the thermal and Dodelson-Widrow distributions [15], $\Delta N_{\rm eff}$ set the ratio of physical mass and the effective mass; $m^{\rm thermal}_{\rm physical} = (\Delta N_{\rm eff})^{-3/4} m^{\rm thermal}_{\rm eff}$ and $m^{\rm DW}_{\rm physical} = (\Delta N_{\rm eff})^{-1} m^{\rm DW}_{\rm eff}$ (see, e.g., [25]). On the other hand, as seen from (27) $\Delta N_{\rm eff}$ is set by the branching ratio, while $w_{\rm sp}$ has also got dependence of the mass and lifetime of the decaying particle (34). This makes $m_{\rm eff}$ and $\Delta N_{\rm eff}$ decoupled. This decoupling is essentially what allows for greater values of mass of our hot dark matter to be consistent with the data.

(ii) Another interesting feature is the ℓ dependence of on the effects on the CMB. For CMB the main effect comes from $\Delta N_{\rm eff}$ as it changes the Hubble expansion rate prior to photon decoupling [88] which changes the silk damping scale. This effect shows up in higher ℓ (small scales) of CMB anisotropy power spectra which is evident from Fig. 6. We see that lower the mass of our DM particle, higher is the effect in small scale as expected. Whereas there is another subtle effect when one introduces interacting dark radiation or nonthermal dark radiation. Free-streaming hot DM travel supersonically through the photon-baryon plasma at early times, hence gravitationally pulling photon-baryon wave-fronts slightly ahead of where they would be in the absence of neutrinos. As a result, the free-streaming neutrinos imprint a net phase shift in the CMB power spectra toward larger scales (smaller ℓ), as well as a suppression of its amplitude [31]. In our case when we keep $\Delta N_{\rm eff}$ more or less fixed given by Planck bound and as we vary hot DM mass, the distribution function also (as well as hot DM velocity) changes and the effects shows up in small ℓ values of CMB spectra. We can find this effect in the left panel of from Fig. 6, where in small ℓ values we see the deviations for different choices of mass of our hot DM particle. This, we find to be a very interesting effect and a detailed MCMC statistical analysis (which is work in progress) will make it clearer whether it can be detected by upcoming CMB and LSS experiments.

IV. DISCUSSION AND FUTURE DIRECTIONS

We have considered hot dark matter produced from decays in a universe transiting from matter domination to radiation domination. Such epochs can occur naturally during the perturbative decay of the inflaton or as a result of vacuum misalignment of moduli fields. We have taken into account the characteristic momentum distribution of hot dark matter particles produced in this manner and obtained their effects on the CMB and LSS making use of CLASS. Our analysis has revealed interesting features such as higher values of hot dark matter mass being consistent with the linear matter power spectra and corresponding cosmological observations like Wiggle-Z. We have also found features in the CMB at low ℓ potentially related to the phase difference appearing due to supersonic transmission of hot dark matter through the photon-baryon plasma before they turn nonrelativistic. Another interesting feature of our results is the crossover of the light blue curve to the region above the black curve (which corresponds to the case with no sterile particles) at very small scales in lower right panel of Fig. 6. Now to understand why it slightly overshoots in small scales needs rigorous study of the evolution of gravitational potential in the radiation domination era in presence of the new particle and a detailed MCMC simulation within the multiparameter space which is beyond the scope of this paper. Intuitively we feel that the evolution of gravitational potential depends on when exactly our DM sterile particle becomes nonrelativistic (which is also function of τ along with other parameters) and determines the actual shape of power spectra. We believe that a detailed study of results of an MCMC analysis can shed light on this and leave it for future study.

As mentioned above, a detailed MCMC statistical analysis to gain a better understanding of the cosmological implications is under progress. Other than this, there are many interesting avenues that can be pursued with the nonthermal distribution function. Cosmology has entered a high precision era not only with respect to the CMB but also through nonlinear structure formation. It will be really interesting to study structure formation with a nonthermal distribution function like ours. As has been pointed out in [92], the velocity phase space distribution plays a crucial role for nonlinear structure formation in the presence of hot DM. Another future avenue is the study of implications of the presence of such relativistic hot DM particles and the corresponding extra radiation like degrees of freedom for the Hubble anomaly [93]. For a standard neutrinolike particle, when one tries to address the Hubble anomaly by increasing the effective amount of radiation, it indeed tends to relax the tension but only partially [94]. The reason for this is that an effective increase in the number of thermal neutrinolike particles makes the CMB high ℓ power deviate [31] from the observed Planck value. It will be very interesting to see if this nonthermal distribution function could help us with the high ℓ discrepancy. This is work in progress and will be reported in the near future.

In this paper, we have not made an attempt to connect to the short base line anomaly [95], but it is worth pointing out that nontrivial momentum distribution functions as well as decay products might have implications for these anomalies. In our case, if the inflaton/moduli decay to

[7]Recall that the effective mass of a sterile species X is defined by $m^X_{\rm eff} = \Omega_X h^2 94.05$ eV.

intermediate mass sterile states which then decay into eV sterile dark radiation, the idea presented in [33] can be relevant. We leave such a study for future work.

Our set up can be easily extended for warm dark matter [87]—that is a scenario where the mass of the sterile particle is much higher (of the order of KeV). The new distribution function will give rise to new results for WDM from N-body simulations due to changes in the velocity phase space distribution[8] [96] and new constraints on WDM mass from the Lyman-alpha forest [97] and Milky Way (MW) satellites [98,99]. Again, work in this direction is in progress.

Finally, there is lot of optimism that near future experiments will be able to distinguish or detect hot dark matter candidates with different particle physics origin (see, e.g., [100]). For this, understanding the subtle effects which different hot DM particle imprint on CMB power spectra (for our case low ℓ phase shift, high ℓ suppression) that could be measured by CMB-S4 [101] experiments is very important. The same is true for ongoing or upcoming LSS experiments like BOSS [102], DESI [103], EUCLID [104] DES [105] and KiDS [106] which will measure the linear matter power spectra with high accuracy and may be able to distinguish between thermal and nonthermal suppression. It will be very interesting see if our model can also relax recent σ_8 anomaly between CMB and weak lensing results. The present work together with the ongoing MCMC analysis should provide an interesting theory input for all of this.

[8]It will be very interesting to see if the effect of free-streaming is reduced or enhanced in comparison with similar WDM mass produced by standard mechanism such as in [15]. Assuming WDM becomes nonrelativistic in the radiation dominated epoch, in the approximation $\tau \gg t_{\rm nr}$ ($t_{\rm nr}$ being the time that the dark matter particle go nonrelativistic), free streaming length is known to scale as $t_{\rm nr}/a_{\rm nr}$. The results in Sec. II give

$$\frac{t_{\rm nr}}{a_{\rm nr}} \propto \frac{m_\varphi (M_{\rm pl}\tau)^{1/2}}{m_{\rm sp} T_{\rm cmb}}.$$

So we see that depending on τ and $m_{\rm sp}$ we can obtain various values of the free streaming length.

ACKNOWLEDGMENTS

We thank Vivian Poulin and Arka Banerjee for comments on the manuscript and Shiv Sethi, Shouvik Roy Choudhury and Raj Gandhi for useful suggestions. S. B. is supported by postdoctoral fellowship from Physical Research Laboratory, India. Work of M. R. G. is supported by the Department of Science and Technology, Government of India under the Grant Agreement No. IF18-PH-228 (INSPIRE Faculty Award). A. M. is supported in part by the SERB, DST, Government of India by the Grant No. MTR/2019/000267. K. D. is supported in part by the Grant No. MTR/2019/000395, funded by the DST, Govt of India. A. M. would like to thank the Department of Physics, National Taiwan University for hospitality. S. D. acknowledges SERB Grant No. CRG/2019/006147. S. B. and M. R. G. acknowledge the hospitality of the Harish-Chandra Research Institute during the early stages of this project.

[1] J. Silk *et al.*, *Particle Dark Matter: Observations, Models and Searches* (Cambridge University Press, Cambridge, England, 2010).
[2] V. Mukhanov, *Physical Foundations of Cosmology* (Cambridge University Press, Oxford, 2005).
[3] G. Coughlan, W. Fischler, E. W. Kolb, S. Raby, and G. G. Ross, Cosmological problems for the polonyi potential, Phys. Lett. **131B**, 59 (1983).
[4] B. de Carlos, J. Casas, F. Quevedo, and E. Roulet, Model independent properties and cosmological implications of the dilaton and moduli sectors of 4-d strings, Phys. Lett. B **318**, 447 (1993).
[5] T. Banks, D. B. Kaplan, and A. E. Nelson, Cosmological implications of dynamical supersymmetry breaking, Phys. Rev. D **49**, 779 (1994).
[6] M. Cicoli, K. Dutta, A. Maharana, and F. Quevedo, Moduli vacuum misalignment and precise predictions in string inflation, J. Cosmol. Astropart. Phys. 08 (2016) 006.
[7] G. Kane, K. Sinha, and S. Watson, Cosmological moduli and the post-inflationary universe: A critical review, Int. J. Mod. Phys. D **24**, 1530022 (2015).
[8] R. Allahverdi *et al.*, The first three seconds: A review of possible expansion histories of the Early Universe, Open J. Astrophys. **4** (2021), https://doi.org/10.21105/astro.2006.16182.
[9] J. Halverson and P. Langacker, TASI lectures on remnants from the string landscape, *Proc. Sci.*, TASI2017 (2018) 019 [arXiv:1801.03503].
[10] R. J. Scherrer and M. S. Turner, Primordial nucleosynthesis with decaying particles. 1. Entropy producing decays. 2. Inert decays, Astrophys. J. **331**, 19 (1988).
[11] J. P. Conlon and M. C. D. Marsh, The cosmophenomenology of axionic dark radiation, J. High Energy Phys. 10 (2013) 214.
[12] J. Lesgourgues, The cosmic linear anisotropy solving system (CLASS) I: Overview, arXiv:1104.2932.

[13] J. Lesgourgues and T. Tram, The cosmic linear anisotropy solving system (CLASS) IV: Efficient implementation of noncold relics, J. Cosmol. Astropart. Phys. 09 (2011) 032.

[14] J. Lesgourgues and T. Tram, The cosmic linear anisotropy solving system (CLASS) IV: Efficient implementation of noncold relics, J. Cosmol. Astropart. Phys. 09 (2011) 032.

[15] S. Dodelson and L. M. Widrow, Sterile Neutrinos as Dark Matter, Phys. Rev. Lett. **72**, 17 (1994).

[16] R. Valdarnini, T. Kahniashvili, and B. Novosyadlyj, Large scale structure formation in mixed dark matter models with a cosmological constant, Astron. Astrophys. **336**, 11 (1998), arXiv:astro-ph/9804057.

[17] A. Boyarsky, J. Lesgourgues, O. Ruchayskiy, and M. Viel, Realistic Sterile Neutrino Dark Matter with keV Mass Does Not Contradict Cosmological Bounds, Phys. Rev. Lett. **102**, 201304 (2009).

[18] F. Bezrukov, H. Hettmansperger, and M. Lindner, keV sterile neutrino dark matter in gauge extensions of the standard model, Phys. Rev. D **81**, 085032 (2010).

[19] K. Petraki and A. Kusenko, Dark-matter sterile neutrinos in models with a gauge singlet in the Higgs sector, Phys. Rev. D **77**, 065014 (2008).

[20] M. Laine and M. Shaposhnikov, Sterile neutrino dark matter as a consequence of νMSM-induced lepton asymmetry, J. Cosmol. Astropart. Phys. 06 (2008) 031.

[21] K. Abazajian, Linear cosmological structure limits on warm dark matter, Phys. Rev. D **73**, 063513 (2006).

[22] V. Iršič *et al.*, New constraints on the free-streaming of warm dark matter from intermediate and small scale lyman-α forest data, Phys. Rev. D **96**, 023522 (2017).

[23] K. N. Abazajian and A. Kusenko, Hidden treasures: Sterile neutrinos as dark matter with miraculous abundance, structure formation for different production mechanisms, and a solution to the σ_8 problem, Phys. Rev. D **100**, 103513 (2019).

[24] R. Samanta, A. Biswas, and S. Bhattacharya, Non-thermal production of lepton asymmetry and dark matter in minimal seesaw with right handed neutrino induced Higgs potential, J. Cosmol. Astropart. Phys. 01 (2021) 055.

[25] N. Aghanim *et al.* (Planck Collaboration), Planck 2018 results. VI. Cosmological parameters, Astron. Astrophys. **641**, A6 (2020).

[26] S. Das and P. Chanda, Degenerate dark matter micronuggets from eV sterile states and the Hubble tension, arXiv:2005.11889.

[27] S. Das and N. Weiner, Late forming dark matter in theories of neutrino dark energy, Phys. Rev. D **84**, 123511 (2011).

[28] A. A. Aguilar-Arevalo *et al.*, Significant Excess of Electronlike Events in the MiniBooNE Short-Baseline Neutrino Experiment, Phys. Rev. Lett. **121**, 221801 (2018).

[29] M. Aartsen *et al.* (IceCube Collaboration), Search for sterile neutrino mixing using three years of IceCube DeepCore data, Phys. Rev. D **95**, 112002 (2017).

[30] P. Adamson *et al.* (NOvA Collaboration), Search for active-sterile neutrino mixing using neutral-current interactions in NOvA, Phys. Rev. D **96**, 072006 (2017).

[31] C. D. Kreisch, F.-Y. Cyr-Racine, and O. Doré, The neutrino puzzle: Anomalies, interactions, and cosmological tensions, Phys. Rev. D **101**, 123505 (2020).

[32] B. Dasgupta and J. Kopp, Cosmologically Safe eV-Scale Sterile Neutrinos and Improved Dark Matter Structure, Phys. Rev. Lett. **112**, 031803 (2014).

[33] M. Dentler, I. Esteban, J. Kopp, and P. Machado, Decaying sterile neutrinos and the short baseline oscillation anomalies, Phys. Rev. D **101**, 115013 (2020).

[34] S. Dodelson, A. Melchiorri, and A. Slosar, Is Cosmology Compatible with Sterile Neutrinos?, Phys. Rev. Lett. **97**, 041301 (2006).

[35] M. A. Acero and J. Lesgourgues, Cosmological constraints on a light nonthermal sterile neutrino, Phys. Rev. D **79**, 045026 (2009).

[36] S. Hannestad, I. Tamborra, and T. Tram, Thermalisation of light sterile neutrinos in the early universe, J. Cosmol. Astropart. Phys. 07 (2012) 025.

[37] I. M. Oldengott, G. Barenboim, S. Kahlen, J. Salvado, and D. J. Schwarz, How to relax the cosmological neutrino mass bound, J. Cosmol. Astropart. Phys. 04 (2019) 049.

[38] J. Hasenkamp and J. Kersten, Dark radiation from particle decay: Cosmological constraints and opportunities, J. Cosmol. Astropart. Phys. 08 (2013) 024.

[39] J. Hasenkamp, Daughters mimic sterile neutrinos (almost!) perfectly, J. Cosmol. Astropart. Phys. 09 (2014) 048.

[40] S. Roy Choudhury and S. Choubey, Constraining light sterile neutrino mass with the BICEP2/Keck Array 2014 B-mode polarization data, Eur. Phys. J. C **79**, 557 (2019).

[41] J. F. Beacom, N. F. Bell, and S. Dodelson, Neutrinoless Universe, Phys. Rev. Lett. **93**, 121302 (2004).

[42] P. Crotty, J. Lesgourgues, and S. Pastor, Current cosmological bounds on neutrino masses and relativistic relics, Phys. Rev. D **69**, 123007 (2004).

[43] A. Cuoco, J. Lesgourgues, G. Mangano, and S. Pastor, Do observations prove that cosmological neutrinos are thermally distributed?, Phys. Rev. D **71**, 123501 (2005).

[44] M. Cirelli and A. Strumia, Cosmology of neutrinos and extra light particles after WMAP3, J. Cosmol. Astropart. Phys. 12 (2006) 013.

[45] G. F. Giudice, E. W. Kolb, A. Riotto, D. V. Semikoz, and I. I. Tkachev, Standard model neutrinos as warm dark matter, Phys. Rev. D **64**, 043512 (2001).

[46] G. Gelmini, S. Palomares-Ruiz, and S. Pascoli, Low Reheating Temperature and the Visible Sterile Neutrino, Phys. Rev. Lett. **93**, 081302 (2004).

[47] S. Dodelson and L. M. Widrow, Sterile-Neutrinos as Dark Matter, Phys. Rev. Lett. **72**, 17 (1994).

[48] S. Colombi, S. Dodelson, and L. M. Widrow, Large scale structure tests of warm dark matter, Astrophys. J. **458**, 1 (1996).

[49] G. Gelmini, E. Osoba, S. Palomares-Ruiz, and S. Pascoli, MeV sterile neutrinos in low reheating temperature cosmological scenarios, J. Cosmol. Astropart. Phys. 10 (2008) 029.

[50] S. Hannestad, A. Mirizzi, and G. Raffelt, New cosmological mass limit on thermal relic axions, J. Cosmol. Astropart. Phys. 07 (2005) 002.

[51] S. Hannestad, A. Mirizzi, G. G. Raffelt, and Y. Y. Y. Wong, Cosmological constraints on neutrino plus axion hot dark matter: Update after WMAP-5, J. Cosmol. Astropart. Phys. 04 (2008) 019.

[52] P. Crotty, J. Lesgourgues, and S. Pastor, Measuring the cosmological background of relativistic particles with WMAP, Phys. Rev. D **67**, 123005 (2003).
[53] S. Hannestad, Neutrino mass bounds from cosmology, Nucl. Phys. B, Proc. Suppl. **145**, 313 (2005).
[54] S. H. Hansen, G. Mangano, A. Melchiorri, G. Miele, and O. Pisanti, Constraining neutrino physics with BBN and CMBR, Phys. Rev. D **65**, 023511 (2001).
[55] R. Trotta and A. Melchiorri, Indication for Primordial Anisotropies in the Neutrino Background from WMAP and SDSS, Phys. Rev. Lett. **95**, 011305 (2005).
[56] A. D. Dolgov, S. H. Hansen, and A. Yu. Smirnov, Neutrino statistics and big bang nucleosynthesis, J. Cosmol. Astropart. Phys. 06 (2005) 004.
[57] P. Adhya, D. R. Chaudhuri, and S. Hannestad, Late-time entropy production from scalar decay and relic neutrino temperature, Phys. Rev. D **68**, 083519 (2003).
[58] S. Hannestad, What is the lowest possible reheating temperature?, Phys. Rev. D **70**, 043506 (2004).
[59] S. Hannestad, Probing neutrino decays with the cosmic microwave background, Phys. Rev. D **59**, 125020 (1999).
[60] T. Brinckmann, D. C. Hooper, M. Archidiacono, J. Lesgourgues, and T. Sprenger, The promising future of a robust cosmological neutrino mass measurement, J. Cosmol. Astropart. Phys. 01 (2019) 059.
[61] A. Boyle and E. Komatsu, Deconstructing the neutrino mass constraint from galaxy redshift surveys, J. Cosmol. Astropart. Phys. 03 (2018) 035.
[62] R. Allison, P. Caucal, E. Calabrese, J. Dunkley, and T. Louis, Towards a cosmological neutrino mass detection, Phys. Rev. D **92**, 123535 (2015).
[63] S. Mishra-Sharma, D. Alonso, and J. Dunkley, Neutrino masses and beyond- Lambda-CDM cosmology with LSST and future CMB experiments, Phys. Rev. D **97**, 123544 (2018).
[64] S. Hannestad and G. Raffelt, Cosmological mass limits on neutrinos, axions, and other light particles, J. Cosmol. Astropart. Phys. 04 (2004) 008.
[65] J. Morais, M. Bouhmadi-López, and S. Capozziello, Can $f(R)$ gravity contribute to (dark) radiation?, J. Cosmol. Astropart. Phys. 09 (2015) 041.
[66] P. Hernandez, M. Kekic, and J. Lopez-Pavon, $N_{\rm eff}$ in low-scale seesaw models versus the lightest neutrino mass, Phys. Rev. D **90**, 065033 (2014).
[67] K. S. Jeong, M. Kawasaki, and F. Takahashi, Axions as hot and cold dark matter, J. Cosmol. Astropart. Phys. 02 (2014) 046.
[68] P. Di Bari, S. F. King, and A. Merle, Dark radiation or warm dark matter from long lived particle decays in the light of Planck, Phys. Lett. B **724**, 77 (2013).
[69] C. Brust, D. E. Kaplan, and M. T. Walters, New light species and the CMB, J. High Energy Phys. 12 (2013) 058.
[70] T. Higaki, K. S. Jeong, and F. Takahashi, A parallel world in the dark, J. Cosmol. Astropart. Phys. 08 (2013) 031.
[71] M. Archidiacono, E. Giusarma, A. Melchiorri, and O. Mena, Neutrino and dark radiation properties in light of recent CMB observations, Phys. Rev. D **87**, 103519 (2013).
[72] S. Hannestad, A. Ringwald, H. Tu, and Y. Y. Y. Wong, Is it possible to tell the difference between fermionic and bosonic hot dark matter?, J. Cosmol. Astropart. Phys. 09 (2005) 014.
[73] M. C. Gonzalez-Garcia, V. Niro, and J. Salvado, Dark radiation and decaying matter, J. High Energy Phys. 04 (2013) 052.
[74] J. L. Menestrina and R. J. Scherrer, Dark radiation from particle decays during big bang nucleosynthesis, Phys. Rev. D **85**, 047301 (2012).
[75] D. Hooper, F. S. Queiroz, and N. Y. Gnedin, Non-thermal dark matter mimicking an additional neutrino species in the Early Universe, Phys. Rev. D **85**, 063513 (2012).
[76] K. N. Abazajian *et al.* (Topical Conveners: K. N. Abazajian, J. E. Carlstrom, A. T. Lee Collaboration), Neutrino physics from the cosmic microwave background and large scale structure, Astropart. Phys. **63**, 66 (2015).
[77] S. Pastor, T. Pinto, and G. G. Raffelt, Relic Density of Neutrinos with Primordial Asymmetries, Phys. Rev. Lett. **102**, 241302 (2009).
[78] M. Lattanzi and J. W. F. Valle, Decaying Warm Dark Matter and Neutrino Masses, Phys. Rev. Lett. **99**, 121301 (2007).
[79] E. Di Valentino, E. Giusarma, O. Mena, A. Melchiorri, and J. Silk, Cosmological limits on neutrino unknowns versus low redshift priors, Phys. Rev. D **93**, 083527 (2016).
[80] J. Hamann and J. Hasenkamp, A new life for sterile neutrinos: resolving inconsistencies using hot dark matter, J. Cosmol. Astropart. Phys. 10 (2013) 044.
[81] J. Hamann, S. Hannestad, G. G. Raffelt, and Y. Y. Wong, Sterile neutrinos with eV masses in cosmology: How disfavoured exactly?, J. Cosmol. Astropart. Phys. 09 (2011) 034.
[82] S. Hannestad, A. Ringwald, H. Tu, and Y. Y. Wong, Is it possible to tell the difference between fermionic and bosonic hot dark matter?, J. Cosmol. Astropart. Phys. 09 (2005) 014.
[83] J. Lesgourgues and S. Pastor, Neutrino cosmology and Planck, New J. Phys. **16**, 065002 (2014).
[84] A. D. Dolgov, Neutrinos in cosmology, Phys. Rep. **370**, 333 (2002).
[85] A. Palazzo, Phenomenology of light sterile neutrinos: A brief review, Mod. Phys. Lett. A **28**, 1330004 (2013).
[86] H. Baer, K.-Y. Choi, J. E. Kim, and L. Roszkowski, Dark matter production in the early Universe: Beyond the thermal WIMP paradigm, Phys. Rep. **555**, 1 (2015).
[87] K. N. Abazajian, Sterile neutrinos in cosmology, Phys. Rep. **711–712**, 1 (2017).
[88] Z. Hou, R. Keisler, L. Knox, M. Millea, and C. Reichardt, How massless neutrinos affect the cosmic microwave background damping tail, Phys. Rev. D **87**, 083008 (2013).
[89] E. W. Kolb and M. S. Turner, *The Early Universe*, Frontiers in Physics (Westview Press, Boulder, CO, 1990), Vol. 69, https://doi.org/10.1201/9780429492860.
[90] M. Cicoli, J. P. Conlon, and F. Quevedo, Dark radiation in LARGE volume models, Phys. Rev. D **87**, 043520 (2013).
[91] B. S. Acharya, M. Dhuria, D. Ghosh, A. Maharana, and F. Muia, Cosmology in the presence of multiple light moduli, J. Cosmol. Astropart. Phys. 11 (2019) 035.
[92] A. E. Bayer, A. Banerjee, and Y. Feng, A fast particle-mesh simulation of non-linear cosmological structure formation

with massive neutrinos, J. Cosmol. Astropart. Phys. 01 (2021) 016.
[93] F. D'Eramo, R. Z. Ferreira, A. Notari, and J. L. Bernal, Hot axions and the H_0 tension, J. Cosmol. Astropart. Phys. 11 (2018) 014.
[94] A. G. Riess *et al.*, A 2.4% determination of the local value of the Hubble constant, Astrophys. J. **826**, 56 (2016).
[95] A. A. Aguilar-Arevalo *et al.*, Event Excess in the MiniBooNE search for $\bar{\nu}_\mu \to \bar{\nu}_e$ Oscillations, Phys. Rev. Lett. **105**, 181801 (2010).
[96] P. Colin, O. Valenzuela, and V. Avila-Reese, On the structure of dark matter halos at the damping scale of the power spectrum with and without relict velocities, Astrophys. J. **673**, 203 (2008).
[97] A. Boyarsky, J. Lesgourgues, O. Ruchayskiy, and M. Viel, Lyman-alpha constraints on warm and on warm-plus-cold dark matter models, J. Cosmol. Astropart. Phys. 05 (2009) 012.
[98] E. Nadler *et al.* (DES Collaboration), Milky Way satellite census. III. Constraints on dark matter properties from observations of Milky Way satellite galaxies, arXiv: 2008.00022.
[99] S. Das and E. O. Nadler, Constraints on the epoch of dark matter formation from Milky Way satellites, Phys. Rev. D **103**, 043517 (2021).
[100] N. DePorzio, W. L. Xu, J. B. Muñoz, and C. Dvorkin, Finding eV-scale light relics with cosmological observables, Phys. Rev. D **103**, 023504 (2021).
[101] K. Abazajian *et al.*, Cmb-s4 decadal survey apc white paper, 2019.
[102] S. Alam, M. Ata, S. Bailey, F. Beutler, D. Bizyaev, J. A. Blazek, A. S. Bolton, J. R. Brownstein, A. Burden, C.-H. Chuang *et al.*, The clustering of galaxies in the completed sdss-iii baryon oscillation spectroscopic survey: Cosmological analysis of the dr12 galaxy sample, Mon. Not. R. Astron. Soc. **470**, 2617 (2017).
[103] A. Aghamousa *et al.* (DESI Collaboration), The desi experiment part I: Science, targeting, and survey design, arXiv:1611.00036.
[104] L. Amendola, S. Appleby, A. Avgoustidis, D. Bacon, T. Baker, M. Baldi, N. Bartolo, A. Blanchard, C. Bonvin *et al.*, Cosmology and fundamental physics with the euclid satellite, Living Rev. Relativity **21**, 2 (2018).
[105] T. Abbott *et al.* (DES Collaboration), Dark Energy Survey year 1 results: Cosmological constraints from galaxy clustering and weak lensing, Phys. Rev. D **98**, 043526 (2018).
[106] H. Hildebrandt *et al.*, KiDS+VIKING-450: Cosmic shear tomography with optical and infrared data, Astron. Astrophys. **633**, A69 (2020).